

Monoclonal antibody to novel cell surface epitope on Hsc70 promotes morphogenesis of bile ducts in newborn rat liver

David R. Mills · Michelle D. Haskell ·
Helen M. Callanan · Donna L. Flanagan ·
Kate E. Brilliant · DongQin Yang · Douglas C. Hixson

Received: 16 October 2008 / Accepted: 19 April 2009 / Published online: 5 May 2009
© Cell Stress Society International 2009

Abstract We previously described a cell surface reactive monoclonal antibody, MAb OC.10, which recognizes an epitope shared by rat fetal liver ductal cells, hepatic progenitor cells, mature cholangiocytes, and hepatocellular carcinomas (HCC). Here, intrasplenic injection of MAb OC.10 into newborn rats was shown by immunofluorescence microscopy to strongly label intrahepatic bile ducts. Furthermore, the in situ labeling of intrahepatic cholangiocytes by injecting MAb OC.10 increased the number of intraportal and intralobular bile ducts with well-defined lumens when compared to IgM-injected control animals. The antigen for MAb OC.10 was identified by mass spectrometry as Hsc70, a constitutively expressed heat shock protein belonging to the HSP70 family. Immunoblot analysis demonstrated that MAb OC.10 reacted with recombinant bovine Hsc70 protein, with protein immunoprecipitated from rat bile duct epithelial (BDE) cell lysates with monoclonal anti-Hsc70 antibody, and with Hsc70-FLAG protein over-expressed in human 293T cells. In addition, Hsc70-specific small interfering RNA reduced the amount of OC.10 antigen expressed in nucleofected BDE cells. Consistent with the specificity of MAb OC.10 for

Hsc70, heat shock did not induce OC.10 expression in BDE cells, a characteristic of Hsp70. Immunofluorescence with BDE cells further suggested that MAb OC.10 binds a novel cell surface epitope of Hsc70. This was in contrast to a commercially available monoclonal anti-Hsc70 antibody that showed strong cytosolic reactivity. These findings demonstrate that presentation of the OC.10 epitope differs between cytosolic and surface forms of Hsc70 and may suggest distinct differences in protein conformation or epitope availability determined in part by protein–protein or protein–lipid interactions. Phage display and pepscan analysis mapped the epitope for MAb OC.10 to the N-terminal 340–384 amino acids of the ATPase domain of rat Hsc70. These findings suggest that MAb OC.10 recognizes an epitope on rat Hsc70 when presented on the cell surface that promotes morphogenic maturation of bile ducts in newborn rat liver. Furthermore, since we have shown previously that the OC.10 antigen is expressed on HCC subpopulations with oval cell characteristics, our current results indicate that Hsc70 has the potential to be expressed on the surface of certain tumor cells.

Keywords Hsc70 · Epitope mapping · Cell surface · Cholangiocyte · Bile duct

D. R. Mills · M. D. Haskell · H. M. Callanan · D. L. Flanagan ·
K. E. Brilliant · D. Yang · D. C. Hixson
Department of Medicine, Division of Hematology and Oncology,
Rhode Island Hospital/The Warren Alpert Medical
School of Brown University,
Providence, RI 02903, USA

D. C. Hixson
e-mail: Douglas_Hixson@Brown.edu

D. R. Mills (✉)
Rhode Island Hospital,
George Building Room 362, 593 Eddy Street,
Providence, RI 02903, USA
e-mail: David_Mills@Brown.edu

Introduction

Hepatocytes are highly differentiated epithelial cells that constitute approximately 80% of the liver. Under conditions of normal tissue renewal and following injury or surgical resection, hepatocytes rapidly proliferate to regenerate a normal functioning liver. However, if the extent of injury is too severe and hepatocyte regeneration is compromised, activation of a biliary stem cell compartment leads to

expansion of a bipotent oval cell population with the capacity for hepatocytic and ductular pathways of differentiation (Sell and Pierce 1994; Coleman et al. 1997; Dabeva et al. 1997; Sell and Ilic 1997). Oval cells are not the only progenitor populations present in adult liver. Four classes of hepatic stem-like cells have been defined in human liver (Sell 1998), one or more of which may correspond to stem-like cells described in normal and injured rat liver (Novikoff et al. 1996; Tateno and Yoshizato 1996; Hixson and Fowler 1997; Gordon et al. 2000; Hixson et al. 2000). These findings led to the conclusion that the liver is populated with bipotent progenitor cells in various states of differentiation or maturation (Sell 1998).

Understanding the molecular basis for differences in origin, phenotype, and differentiation ability of these various progenitors will require comparative analysis of gene expression at both RNA and protein levels. Although valuable information has been obtained by transplantation analysis using fetal liver isolates or subfractions isolated by physical criteria rather than phenotype, informative comparisons at the molecular level will require phenotypically defined cell isolates. In two recent studies, this goal was reached by isolating clonal progenitor cell populations from total fetal liver isolates or isolates depleted of hematopoietic cells (12–14-day fetal livers) and demonstrating that these isolates can be induced to express ductal or hepatocyte antigens *in vitro* (Kubota and Reid 2000). Whether they can undergo complete ductal or hepatocyte differentiation *in vivo* remains to be determined. In this regard, it was reported that progenitors isolated by fluorescence-activated cell sorting (FACS) using anti- α -6 and anti- β -1 integrin antibodies underwent pancreatic, intestinal, hepatocytic, and bile ductal differentiation following transplantation into these organ sites (Suzuki et al. 2002).

A long-term goal in our laboratory has been the identification of surface markers effective for isolating distinct cell subpopulations that arise during differentiation of cholangiocytes, the cells lining the intrahepatic bile ducts. Our interest in cholangiocytes stemmed from previous reports showing that oval cells of ductular origin could undergo ductal or hepatocyte differentiation. In a recent report, we described a panel of monoclonal antibodies (MAbs) recognizing surface markers on fetal cholangiocytes showing expression patterns that defined four stages in cholangiocyte differentiation (Hixson et al. 2000). FACS analysis of cultured cholangiocytes and oval cells labeled by indirect immunofluorescence with these MAbs showed high levels of expression on the cell surface of bile duct epithelial (BDE) cells, a localization that has made this panel of MAbs invaluable for isolating bipotent fetal cholangiocytes (Simper-Ronan et al. 2006). Identification of the proteins recognized by this panel of MAbs has been a major ongoing effort in our laboratory that has

focused on the identification of the antigen defined by the monoclonal antibody OC.10 (MAb OC.10). MAb OC.10 was raised by nude mouse reconstitution against injected colonies of rat oval cells and has been shown to recognize one of the earliest markers on nascent bile ducts that first appear in rat liver around embryonic day 16. The OC.10 antigen is also expressed at high levels by adult rat cholangiocytes, prostate epithelial cells, and hepatocellular carcinomas with mixed oval cell/hepatocyte phenotypes. Reactivity of MAb OC.10 has not been observed against hepatocytes (Hixson et al. 2000). In this report, we present data that identifies OC.10 as an epitope displayed by a surface form of the constitutively expressed heat shock protein, Hsc70. We also demonstrate that intrasplenic injection of MAb OC.10 strongly labels intraportal/intralobular bile ducts also positive for the ductal cytokeratin marker OV-6 (Dunsford et al. 1989; Hixson et al. 2000) and promotes morphogenesis of bile duct structures in newborn rat liver.

Materials and methods

In situ labeling of cholangiocytes with injected MAb OC.10

Timed pregnancy, wild-type Fisher 344 rats were purchased from Harlan (Indianapolis, IN, USA). Animals were fed standard rat chow *ad libitum* and were housed in an alternating 12-h light/dark cycle environment. Newborn Fisher rats were injected into the spleen at 24-h intervals for three consecutive days with 20 μ g of MAb OC.10, MAb OC.5, a control IgM antibody that reacts with the cell surface of cholangiocytes (Hixson et al. 2000), or MAb BD.1, an IgM antibody against a cholangiocyte cytoplasmic protein (Yang et al. 1993a). Five hours after the third injection, livers were excised and frozen in hexane chilled with a dry ice–acetone bath. Serial frozen tissue sections were fixed in ice-cold acetone for 10 min and stained with Alexa Fluor 594 goat anti-mouse IgM secondary antibody (1:400; Invitrogen Corporation, Carlsbad, CA, USA) to observe *in situ* localization of injected MAb OC.10 and MAb OC.5. To identify bile ducts, serial sections from MAb OC.10- and MAb OC.5-injected animals were incubated for 30 min at room temperature with MAb OV-6 (IgG; 1:300 diluted in phosphate-buffered saline (PBS)), an antibody recognizing an epitope shared by cytokeratin 19 (CK19) and CK14 (Dunsford et al. 1989; Bisgaard et al. 1993). After several PBS washes, the sections were incubated at room temperature with goat anti-mouse IgG (Fc; Pierce Chemical Co., Rockford, IL, USA) and Alexa Fluor 594 goat anti-mouse IgM secondary antibodies. The number of OV-6-positive bile ducts with a well-defined lumen was determined for approximately 50 portal areas from each injected animal. Differences between the average

number of lumen positive bile ducts (LPBD) in MAb OC.10 (group A) and MAb OC.5 (group B)-injected animals were tested for statistical significance using Student's *t* test with *P* values less than 0.05 indicating significance. National Institutes of Health guidelines for the care and use of laboratory animals were followed throughout this investigation. All animal protocols carried out in these studies were approved by the Rhode Island Hospital Institutional Animal Care and Use Committee.

Purification of OC.10 antigen

Rat biliary tree isolated following collagenase perfusion of the liver as described by Yang et al. (1993a) was solubilized in 0.5% Triton X-100 with protease inhibitors (Roche Diagnostics Co., Indianapolis, IN, USA) for 2 h at 4°C. Clarified extract was passed over wheat-germ agglutinin coupled to Sepharose at a protein concentration of 5 mg/ml. Flow through was submitted to QA anion exchange chromatography using 20 mM Tris, pH 7.2. The unbound fraction was dialyzed against 10 mM phosphate buffer, pH 6.8 and loaded onto a hydroxyapatite column (Bio-Rad Laboratories, Inc., Hercules, CA, USA). Fractions eluted with a 0.1–0.5-M Na₂PO₄ gradient, pH 6.8, were resolved by sodium dodecyl sulfate polyacrylamide gel electrophoresis (SDS-PAGE) and OC.10-positive fractions identified by immunoblot analysis were pooled, dialyzed against 0.5 mM Tris pH 7.2, and loaded onto a VyDac C4 reverse phase column. Aliquots from fractions containing proteins eluted in a 0–90% gradient of acetonitrile with 0.1% trifluoroacetic acid were dialyzed against 0.5 mM Tris buffer pH 7.2 and subjected to immunoblot analysis as described below. A duplicate gel was stained with Sypro Ruby (Invitrogen Corporation) and a band with an apparent molecular weight identical to the reactive band in immunoblots was excised and submitted to the Yale Cancer Center Mass Spectrometry Resource/W. M. Keck Foundation Biotechnology Resource Laboratory (New Haven, CT, USA) where an in-gel trypsin digest was performed. Tryptic peptides resolved by reverse phase high-performance liquid chromatography (HPLC) were analyzed by electrospray ionization mass spectrometry. Masses of major tryptic peptides were compared to theoretical tryptic peptide profiles for known protein in the OWL protein database using the Profound Server.

Cloning of rat Hsc70

Reverse transcriptase-polymerase chain reaction (RT-PCR) was used to generate a cDNA corresponding to the full-length rat wild-type Hsc70. RT-PCR amplification was performed using oligo dT-primed rat liver RNA and sequence specific primers for Hsc70 containing a 5' *EcoRI*

site and a 3' *BamHI* site. The amplified PCR products were directionally ligated into pFLAG-CMV5a (Sigma-Aldrich Co., St. Louis, MO, USA), which adds a carboxyl-terminal FLAG-tag to the expressed protein.

Cell culture and transient transfections

BDE4, a continuous line of rat liver bile duct epithelial cells, was derived and cultured as described (Yang et al. 1993b). Human 293T cells were cultured in DMEM/F12 media supplemented with 10% FBS and 50 µg/ml gentamicin (Invitrogen Corporation) and incubated at 37°C in a 5% CO₂ humidified atmosphere. For heat shock experiments, BDE4 cells were incubated at 42°C for the indicated times in a 5% CO₂ humidified atmosphere. Human 293T cells were transfected with Hsc70-FLAG constructs using Lipofectamine 2000 as described in the manufacturer's instructions (Invitrogen Corporation). Transiently transfected 293T cells were harvested at 48 h and prepared for immunoprecipitations as described below. For small interfering RNA (siRNA) studies, BDE4 cells were grown to approximately 80% confluence and nucleofected with 21-nucleotide siRNAs using the Amaxa system (Amaxa Inc., Gaithersburg, MD, USA) as described in the manufacturer's instructions using solution V and program X-005. Silencer pre-designed siRNAs targeting rat Hsc70 (heat shock protein 8) were from Ambion Inc. (Austin, TX, USA). The following sequences were used: 5'-GGAAUGUGCUCAUUUUUGATT-3' and 5'-UCAAAAUGAGCACAUUCCTT-3' (siRNA ID #: 52960); 5'-GGUGGAAAUAUUUGCCAAUTT-3' and 5'-AUUGGCAAUUAUUUCCACCTT-3' (siRNA ID #: 52780); 5'-GCUAUGUUGCUUUCACCGATT-3' and 5'-UCGGUGAAAGCAACAUAAGCTC-3' (siRNA ID #: 201029). The Silencer negative control #1 siRNA was used to control for the effects of siRNA delivery. To observe knockdown of OC.10, 5 × 10⁶ cells were nucleofected with siRNA, cultured for 72 h and examined for siRNA effects by immunoblot analysis. Anti-GAPDH antibody (Ambion Inc.) was used to normalize for equal loading of protein, and band densities were determined using Photoshop CS (Adobe, San Jose, CA, USA). The relative intensity for each sample band was determined by dividing the absolute intensity of each sample band by the absolute intensity of the GAPDH loading control. Statistical analysis was performed using a nonparametric, paired *t* test with GraphPad Prism software (GraphPad Software, Inc., La Jolla, CA, USA). *P* < 0.05 was considered to be statistically significant.

Immunofluorescent microscopy

BDE4 cells were seeded in two-well permanox chamber slides (Nalge Nunc International, Rochester, NY, USA) at a

density of 1×10^5 cells/ml and incubated for 48–72 h in a 5% CO₂ humidified chamber. Cells were washed three times in PBS and fixed and permeabilized for 15 min in ice-cold acetone. Live and acetone fixed BDE4 cells were blocked for 10 min in 1% bovine serum albumin (BSA)/PBS with 10% normal goat serum (Sigma-Aldrich Co.). Primary and secondary antibodies were diluted in 1% BSA/PBS with 10% normal goat serum and incubated sequentially with cells for 45 min at room temperature. Cells were examined by fluorescence microscopy using a Nikon Eclipse E800 microscope (Nikon Instruments, Inc., Melville, NY, USA). Antibody dilutions were as follows: MAb OC.10 (IgM), 1:500; monoclonal anti-Hsc70 (IgG; Stressgen Bioreagents, Victoria, British Columbia), 1:100; Alexa Fluor 488 goat anti-mouse IgG and Alexa Fluor 594 goat anti-mouse IgM secondary antibodies (Invitrogen Corporation), 1:400.

Immunoprecipitations

Cells were lysed in situ with NP-40 lysis buffer (1% NP-40, 50 mM Tris, pH 7.5, 150 mM NaCl, and 1 Complete Protease Inhibitor tablet [Roche Diagnostics Co.]) or with the M-PER Mammalian Protein Extraction Reagent (Pierce Chemical Co.) as described in the manufacturer's instructions. Detergent insoluble material was removed by centrifugation at 14,000 rpm for 15 min at 4°C. For Hsc70 immunoprecipitations, 500 µg total protein was incubated with 5 µg of monoclonal anti-Hsc70 or MAb OC.10 (IgM) for 1 h at 4°C. Lysates were incubated with rec-Protein G-Sepharose 4B conjugate (Zymed Laboratories Inc., San Francisco, CA) or rat anti-mouse IgM Dynabeads M-450 (DynaL Biotech ASA, Oslo, Norway) for 1 h at 4°C. To immunoprecipitate Hsc70-FLAG tagged protein, 500 µg of total 293T cell lysate was incubated with anti-FLAG M2 agarose according to the manufacturer's instructions (Sigma). Following five washes with RIPA buffer (50 mM Tris, pH 7.5, 150 mM NaCl, 0.5% sodium deoxycholate, 1% Triton X-100, 0.1% SDS, and 1 Complete Protease Inhibitor tablet), the Protein G-Sepharose 4B beads were suspended in nonreducing SDS sample buffer (Bio-Rad Laboratories) and boiled for 5 min. The anti-FLAG M2 agarose was suspended in reducing SDS-PAGE sample buffer and boiled for 5 min.

Biotinylation of cell surface proteins

BDE4 cells were cultured to 60% confluence, washed with PBS, and biotinylated with 0.5 mg/ml Sulfo-NHS-LC-LC Biotin (Pierce Chemical Co.) in PBS for 30 min at 4°C. Cells were washed with 50 mM glycine/PBS for 15 min at 4°C to quench unreacted biotin. Cells harvested using nonenzymatic cell dissociation solution (Sigma-Aldrich Co.) were lysed with M-PER Mammalian Protein Extrac-

tion Reagent (Pierce Chemical Co.). Lysate was incubated with immobilized neutravidin biotin-binding beads (Pierce Chemical Co.) for 2 h at 4°C. Neutravidin-precipitated proteins released by boiling in SDS-PAGE sample buffer for 5 min were separated by SDS-PAGE and visualized using Gelcode Blue Stain Reagent (Pierce Chemical Co.). Recombinant Hsc70 protein was used as a size standard to excise a band in the range of 70 kDa. Biotinylated cell surface proteins were prepared and analyzed by liquid chromatography electrospray ionization tandem mass spectrometry (LC-ESI-MS/MS) on a QSTAR XL mass spectrometer (Applied Biosystems, Framingham, MA, USA and Sciex, Concord, Ontario, Canada) at the Center of Biomedical Research Excellence (COBRE) Proteomics Core Facility (Providence, RI, USA) as described (Clifton et al. 2006).

Western blotting

Proteins separated by 7.5% SDS-PAGE were transferred onto nitrocellulose (Trans-Blot Transfer Medium, Bio-Rad Laboratories) and immunoblotted as described (Yang et al. 1993a). Reactivity was visualized by chemiluminescence with SuperSignal West Pico chemiluminescent substrate according to the manufacturer's instructions (Pierce Chemical Co.). Recombinant bovine Hsc70 and rat Hsp70 proteins were obtained from Stressgen Bioreagents, Victoria, British Columbia. Antibody dilutions were as follows: monoclonal OC.10, 1:1,000; monoclonal anti-Hsc70, 1:1,000; polyclonal anti-Hsp70 (IgG; Stressgen, Victoria, BC, Canada), 1:5,000; monoclonal anti- α -tubulin (IgG; Calbiochem Inc., San Diego, CA, USA), 1:1,000; polyclonal anti-actin (IgG; Sigma-Aldrich Co.), 1:500; monoclonal anti-GAPDH (IgG; Ambion Inc.), 1:50,000; monoclonal anti-FLAG M2 antibody, 1:1,000; and goat anti-mouse IgM, goat anti-mouse IgG, and goat anti-Rabbit Ig horseradish peroxidase (HRP)-conjugated secondary antibodies (Biosource, Camarillo, CA, USA), 1:25,000.

Epitope mapping using phage display and peptide arrays

Initial epitope mapping studies were performed with the Ph.D.-12 Phage Display Peptide Library Kit according to the manufacturer's instructions (New England Biolabs Inc., Ipswich, MA, USA). Briefly, a sterile polystyrene petri dish was coated with antibody by incubating with 150 µg of purified MAb OC.10 in 0.1 M NaHCO₃ (pH 8.6) overnight at 4°C, followed by blocking in 0.1 M NaHCO₃ (pH 8.6) containing 5 mg/ml of BSA at 4°C for 1 h, and six washes with TBST (TBS + 0.1% [v/v] Tween 20). The phage library (4×10^{10} /ml TBST) was then added to the blocked plate and incubated at room temperature for 1 h. The plate was washed ten times with TBST, the antibody-bound

phage was eluted with 0.2 M glycine-HCl (pH 2.2), and the collected eluate was neutralized with 1 M Tris-HCl (pH 9.1). Following amplification according to the manufacturer's protocol, the eluted phage was taken through three additional cycles of biopanning and amplification to enrich for the phages with the highest affinity. Ten clones were submitted for DNA sequencing to the W.M. Keck Biotechnology laboratory at Yale University (New Haven, CT, USA) to determine the nucleotide sequences encoding the phage displayed peptides. Epitope mapping was also performed using a PepSpots peptide array spanning amino acids 340–410 of rat Hsc70. Peptides reactive with MAb OC.10 were identified using the manufacturer's protocol (JPT Peptide Technologies GmbH, Berlin, Germany). Briefly, a membrane containing 30 overlapping 13-mer PepSpots peptides was rinsed in methanol for 5 min, washed in TBS (50 mM Tris, 137 mM NaCl, 2.7 mM KCl, pH 8.0) for 10 min and blocked at room temperature for 2 h with SuperBlock Blocking Buffer in TBS (Pierce Chemical Co.). Purified MAb OC.10 was conjugated to HRP using the Lightning-Link HRP Conjugation Kit as described by the manufacturer's instructions (Innova Biosciences Ltd., Cambridge, UK) and 1 µg/ml of labeled antibody was incubated for 2 h at room temperature with the blocked PepSpots membrane. Reactivity was visualized by chemiluminescence with SuperSignal West Pico Chemiluminescent Substrate according to the manufacturer's protocol (Pierce Chemical Co.).

Results

In situ labeling of cholangiocytes with MAb OC.10 promotes ductal morphogenesis

Our laboratory has successfully used MAb OC.10 in combination with other antibodies to isolate antigenically defined subpopulations of OC.10-positive fetal cholangiocytes (Simper-Ronan et al. 2006). In the course of the present investigations, we discovered that within an hour of injection of MAb OC.10 into the spleen of newborn Fisher rats, the antibody appeared exclusively on the surface of intraportal/intralobular bile ducts where it remained for at least 5 h post-injection (not shown). Our ability to label bile ducts in situ with MAb OC.10 provided a means to determine if antibody binding would elicit a biological response. As shown in Fig. 1, injection of MAb OC.10 for three consecutive days resulted in strong and highly specific labeling of intraportal/intralobular ducts (Fig. 1a). In contrast, very few bile ducts were labeled in situ by MAb OC.5, although some larger ducts did exhibit weak reactivity (Fig. 1c). As expected, bile ducts were also negative for MAb BD.1, a cytoplasmic marker found on

bile ducts but not oval cells (not shown; Yang et al. 1993b). These findings showed that the binding of MAb OC.10 was specific for the surface exposed Hsc70 epitope and was not the result of nonspecific adhesion of IgM antibody to intrahepatic bile ducts. To confirm that injected MAb OC.10 was labeling bile ducts, serial cryosections from MAb OC.10- and OC.5-injected animals were incubated with MAb OV-6, a biliary marker that reacts with CK19 and CK14 (Dunsford et al. 1989; Hixson et al. 2000). Primary staining was followed with a cocktail of anti-IgM and IgG secondary antibodies to compare the labeling reactivity of the injected IgM primary antibodies with OV-6 expression. As shown in Fig. 1b, the reactivity profile of injected MAb OC.10 was restricted to OV-6-positive ducts.

During the early post-partum period, the biliary system in the liver continues to undergo morphological, phenotypic, and functional maturation. Bile canaliculi retain the distended morphology characteristic of late gestation fetal liver. Bile ducts often lack a clearly defined central lumen and have not yet begun to express surface markers such as OC.4 that are characteristic of mature ducts (Hixson et al. 2000). To determine if in situ labeling of ducts with MAb OC.10 would stimulate their morphological or phenotypic maturation, serial cryosections from MAb OC.10-injected newborn rats were labeled with MAb OC.4 that first appears on cholangiocytes at 2–3 weeks after birth (Hixson et al. 2000). Extensive analysis of serial frozen sections did not reveal any OC.4-positive bile ducts in newborn rats injected with MAbs OC.10, OC.5, BD.1, or uninjected controls (data not shown), indicating that MAb OC.10 did not accelerate phenotypic maturation as defined by the appearance of OC.4. To determine if injected antibodies had an effect on morphogenic maturation, serial cryosections were labeled with MAb OV-6 and the number of LPBD was determined for 252 or 169 nonoverlapping portal areas from five MAb OC.10-injected or three MAb OC.5-injected animals, respectively. Injection of MAb OC.10 significantly increased the number of well-defined LPBD per portal area (Fig. 1a, b) relative to MAb OC.5-injected control animals (Fig. 1c, d). As summarized in Table 1, this analysis yielded an average of 3 LPBD/portal area in MAb OC.10-injected animals, a frequency that was significantly higher ($P < 0.05$) than the average of 1.1 LPBD/portal area in MAb OC.5-injected animals. The morphogenic changes induced in situ by MAb OC.10 suggest that the reactive epitope is located in a functional domain of Hsc70 that is activated by antibody binding.

Mass spectrometry identified the OC.10 antigen as Hsc70

As a first step to identify the protein recognized by MAb OC.10, we initiated experiments to purify the reactive antigen. After numerous unsuccessful attempts to affinity

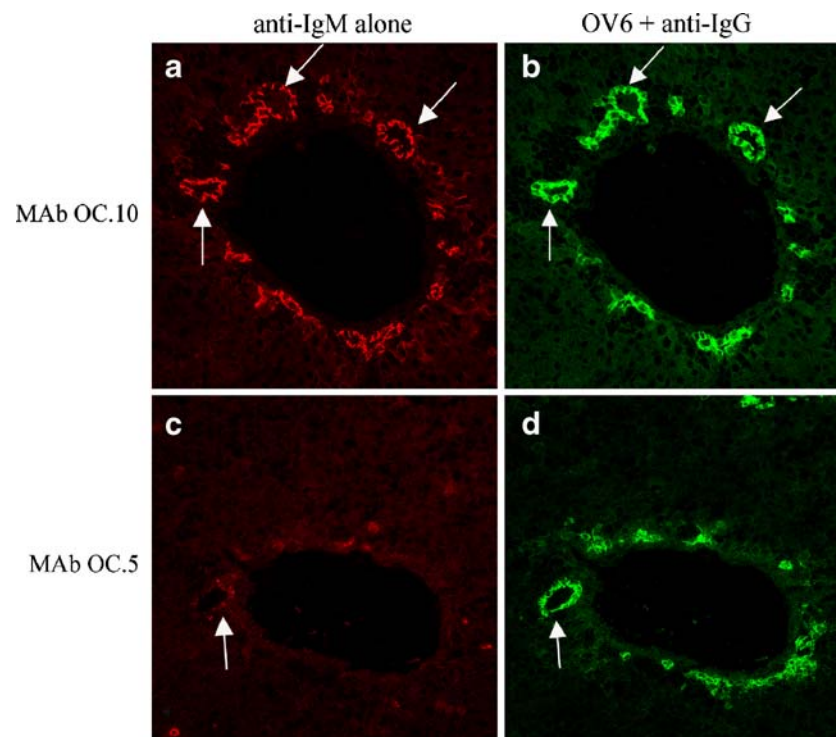


Fig. 1 Injected MAb OC.10 promotes bile duct formation in newborn rat liver. MAb OC.10 (20 μ g) or control IgM MAb OC.5 was injected into the spleen of newborn Fisher rats at 24-h intervals for 3 days. Five hours after the third injection, livers were excised, frozen, sectioned, and stained with Alexa Fluor 594 goat anti-mouse IgM secondary antibody to determine if injected antibody labeled intrahepatic ducts. As shown, injection of MAb OC.10 resulted in strong labeling of intrahepatic bile ducts (**a**). In contrast, MAb OC.5 did not label ductal cells (**c**). To view bile ducts, tissue sections were stained

with the ductal-specific marker MAb OV-6 (IgG) and a cocktail of anti-IgM and IgG (Fc) secondary antibodies. Well-defined MAb OV-6 + ducts located around portal vein branches were compared between MAb OC.10- and MAb OC.5-injected liver sections. Sections from MAb OC.10-injected animals show that the OC.10 (**a**) and OV-6 (**b**) antigens co-localize and that MAb OC.10 promotes bile duct formation as evidenced by the significantly ($P < 0.05$) higher frequency of defined bile ducts (*arrows*) per portal vein area as compared to MAb OC.5-injected animals (**d**)

Table 1 Effect of MAb OC.10 on intrahepatic ductal morphology, where P represents the total number of portal areas counted, BD represents the total number of defined bile ducts counted, and BD/ P represents the average number of bile ducts per portal area

Treatment	P	BD	BD/ P
MAb OC.10			
Animal 1	44	109	2.5
Animal 2	30	145	4.8
Animal 3	54	132	2.4
Animal 4	69	197	2.9
Animal 5	55	166	3.0
MAb OC.5			
Animal 1	37	73	2.0
Animal 2	60	53	0.9
Animal 3	72	69	1.0

The average BD/ P for MAb OC.10-injected animals was 3.0, a frequency significantly higher ($P < 0.05$) than the average of 1.1 for MAb OC.5-injected animals

purify OC.10, we designed a protocol based on established methods to isolate OC.10 from a Triton X-100 extract of rat biliary tree. The final protocol involved the removal of major contaminants by passing the extract through wheat-germ agglutinin and QA anion exchange columns, which do not bind OC.10, followed by binding to hydroxyapatite and elution with a sodium phosphate gradient. Fractions testing positive by Western blot were pooled and further purified by reverse phase chromatography on a C4 hydrophobic interaction column and SDS-PAGE. A Sypro Ruby band with the same mobility as MAb OC.10 in a duplicate immunoblot was excised, digested in-gel with trypsin, and analyzed by HPLC and tandem mass spectrometry (LC-ESI-MS/MS). LC-ESI-MS/MS analysis indicated that the presumptive OC.10 band contained highly purified Hsc70, a constitutively expressed member of the heat shock protein 70 (HSP70) family. Figure 2 shows the Hsc70 peptides identified from MS analysis of two separate preparations of purified OC.10. The first preparation identified 13

```

1 mskgpavgidlgttyscvqvfqhkgk VEIANDQGNR TTPSYVAFTDTER ligdaak ngva
61 mnptntvfdak rligr rfddavvqsdmk hwpfvmvndagrpkvqvveykgetk sfypeeivs
121 smvltk mk EIAEAYLGK TVTNAVVTVPAYFNDSQR qatk DAGTIAGLNVLRL IINEPTAAA
181 IAYGLDK kvgaernvlfidlgggtfdvsiltiedgifevk STAGDTHLGGEDFDNR mvnh
241 fiaefkrkhkkdisenkravrrlrtacerakrtlssstqasieidslyegidfytsitra
301 r FEELNADLFR gtlpvekalrdakldk SOIHDIVLVGGSTR ipkiqkllqdfngkeln
361 ksinpdeavaygaavqaailsqdkxenvqdlldvtplslgietaggvmtvlkrntti
421 ptk QTOTFTTYSNQPGLIQVYEGER amtkdnnllgk FELTGIPPAPR gvpqievtfdi
481 dangilnvsavdkstgkenkititndkgrlskediermvqeaekykaedekqrdkvsskn
541 slk SYAFNMKATVEDEK lqgkindedkqkildkcneiinwldk NOTAEKEEFEHQOK ele
601 kvcnpiitk lyqsagmpggmpggmpggfpgggappsggassgptieevd
    
```

Fig. 2 Matrix-assisted laser desorption ionization mass spectrometry (MALDI-MS) identified the OC.10 antigen as bovine Hsc70 protein (gi 123644). Two separate MALDI-MS analyses of trypsinized OC.10 protein obtained from Coomassie-stained gels were performed and revealed a number of Hsc70 peptide fragments. The 13 Hsc70 peptide

fragments identified in MALDI-MS analysis 1 are *italicized* and indicated by *uppercase letters*. MALDI-MS analysis 2 identified 17 peptide fragments of Hsc70 that are *italicized and underlined*. Analysis 1 and analysis 2 covered 28% and 34% of the bovine Hsc70 sequence, respectively

peptides that matched bovine Hsc70 (gi 123644) and represented 28% of the protein. The second preparation identified 17 Hsc70 peptides representing 34% of the full-length bovine Hsc70 sequence.

MAb OC.10 reacts with recombinant and immunoprecipitated Hsc70

To verify the identity between OC.10 and Hsc70, the reactivity of MAb OC.10 with recombinant bovine Hsc70 was confirmed by immunoblot analysis. A commercially available anti-Hsc70 antibody was used as a positive control. Because of the high level of sequence homology between Hsc70 and Hsp70 (Tavaria et al. 1996), the

specificity of MAb OC.10 was also tested against recombinant Hsp70 protein. As shown in Fig. 3, MAb OC.10 and the anti-Hsc70 MAb each reacted with recombinant Hsc70 protein (Fig. 3, lanes 1–3) but showed no detectable reactivity against recombinant Hsp70 protein (Fig. 3, lanes 5–7). To further confirm the reactivity of MAb OC.10 with Hsc70, we transiently expressed a rat Hsc70-FLAG tagged expression plasmid in the human 293T cell line. As shown in Fig. 4, immunoblot analysis of the anti-FLAG immunoprecipitate showed that MAb OC.10, commercial anti-Hsc70, and anti-FLAG antibodies all displayed strong reactivity with the FLAG-tagged Hsc70 (Fig. 4, lane 2). No antibody reactivity was observed against immunoprecipitates from negative control 293T lysates (Fig. 4, lane 1).

To obtain further evidence for the specificity of MAb OC.10 for Hsc70, BDE4 lysate was immunoprecipitated with monoclonal anti-Hsc70 antibody. As shown in Fig. 5, MAb OC.10 reacted with a 70-kDa peptide in total BDE4 lysate and in anti-Hsc70 immunoprecipitates. Reactivity was not observed against fractions eluted from lysates

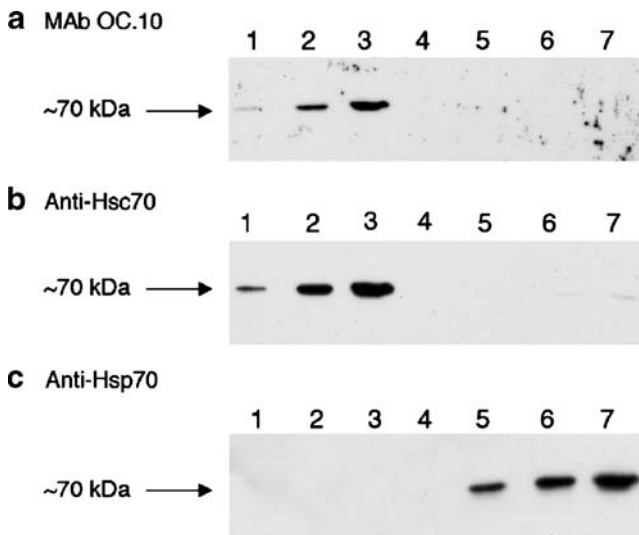


Fig. 3 Immunoblotted MAb OC.10 reacts with Hsc70 protein. Recombinant bovine Hsc70 (lanes 1–3) and recombinant Hsp70 (lanes 5–7) proteins were immunoblotted with MAb OC.10 (a), monoclonal anti-Hsc70 (b), and polyclonal anti-Hsp70 (c). For each protein, 50 ng (lanes 1 and 5), 100 ng (lanes 2 and 6), and 200 ng (lanes 3 and 7) were resolved on 7.5% polyacrylamide gels and transferred onto nitrocellulose. Lane 4 was empty

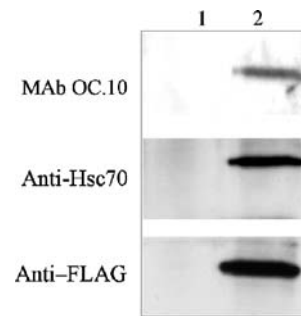


Fig. 4 MAb OC.10 reacts with Hsc70-FLAG protein over-expressed in human 293T cells. An Hsc70-FLAG expression construct was transfected into human 293T cells. Immunoblots of protein immunoprecipitated with anti-FLAG agarose identified an ~70-kDa protein that reacted with MAb OC.10, monoclonal anti-Hsc70, and anti-FLAG antibodies (lane 2). Reactivity was not observed against the immunoprecipitated fraction from nontransfected cell lysates (lane 1) demonstrating specificity for FLAG-tagged Hsc70 in lane 2

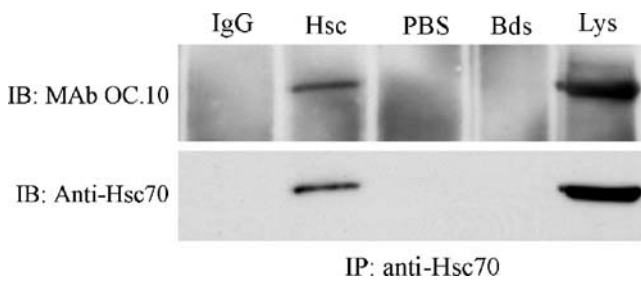


Fig. 5 MAb OC.10 reacts with protein immunoprecipitated with anti-Hsc70 antibody. BDE4 cell extract (500 μ g) prepared in NP-40 lysis buffer with 2 mM ADP was immunoprecipitated with 5 μ g of rat monoclonal anti-Hsc70 (*Hsc*) or 5 μ g of control rat IgG (anti-Ras, *IgG*) for 1 h at 4°C. Total cell lysate (20 μ g, *Lys*), monoclonal anti-Hsc70 in PBS (i.e., no cell extract), and precipitate from lysate with beads alone (*Bds*) were loaded as additional controls. The membrane was immunoblotted with OC.10 (*top panel*) and stripped and re-probed with monoclonal anti-Hsc70 (*lower panel*)

incubated with beads alone, anti-Hsc70 antibody in PBS (i.e., no lysate), or a control anti-Ras IgG. Efficient immunoprecipitation of Hsc70 protein was confirmed when the blot was stripped and re-probed with monoclonal anti-Hsc70 antibody.

The OC.10 antigen behaves like Hsc70

The Hsc70 and Hsp70 proteins are differentially regulated with Hsc70 being constitutively expressed and Hsp70 induced by environmental stress (e.g., heat shock; De Maio 1999). To further demonstrate that MAb OC.10 reacted with Hsc70 and not an epitope shared by Hsc70 and Hsp70, we examined the effect of heat shock on protein levels recognized by MAb OC.10. Anti-Hsc70 and anti-Hsp70 antibodies were used to distinguish between constitutive and induced proteins. As shown in Fig. 6, heat treatment of BDE4 cells did not induce an increase in the level of protein recognized by MAb OC.10 or anti-Hsc70 following 42°C heat shock treatments of 0, 2, 6, or 24 h. In contrast, the levels of protein detected by anti-Hsp70 were significantly increased following heat shock treatment.

To further show that the OC.10 antigen is Hsc70, we nucleofected BDE4 cells with rat Hsc70-specific siRNAs, prepared total cell lysates, and tested for expression of the OC.10 antigen and Hsc70 by immunoblot analysis. Of the three Hsc70-specific siRNAs tested, one demonstrated more significant knockdown of Hsc70 levels (siRNA ID #: 52960) than the other two at 72 h post-nucleofection (data not shown). Subsequent Hsc70 knockdown studies were limited to siRNA 52960. Immunoblot analysis showed that siRNA 52960 highly attenuated Hsc70 and OC.10 expression levels as compared with the mock-nucleofected control (Fig. 7), further confirming the specificity of MAb OC.10 for Hsc70 protein.

Immunofluorescent distribution of OC.10 and Hsc70 in BDE4 cell monolayers

We have shown previously that MAb OC.10 reacts specifically with ductal structures in fetal, newborn, and adult rat liver (Hixson et al. 2000). To examine more precisely the subcellular localization of protein epitopes recognized by MAb OC.10 and a commercially available monoclonal anti-Hsc70 antibody, rat BDE4 cells were examined by immunofluorescence microscopy. As shown in Fig. 8a, with acetone fixed cells, MAb OC.10 exhibited intense and uniform plasma membrane reactivity with minimal levels of reactivity against cytosolic Hsc70. In contrast, monoclonal anti-Hsc70 showed a distinct absence of detectable membrane reactivity and a pronounced cytosolic and nuclear staining, a well-known distribution pattern for Hsc70 (Tsukahara and Maru 2004). Co-localization of MAb OC.10 and anti-Hsc70 demonstrates the specificity for membrane and cytosolic epitopes, respectively. We next examined MAb OC.10 and anti-Hsc70 reactivity against live, nonpermeabilized BDE4 cells. As shown in Fig. 8b, reactivity of MAb OC.10 was limited to the leading edge of nonconfluent cell colonies where it appeared to be polarized towards the outer membrane surface. MAb OC.10 reactivity was not observed in other membrane domains and was absent or weakly expressed on cells in the interior of each colony. This was in contrast to the strong surface membrane reactivity observed on all cells following acetone fixation. Reactivity was not observed on live cells with the commercial monoclonal anti-Hsc70 antibody (not shown).

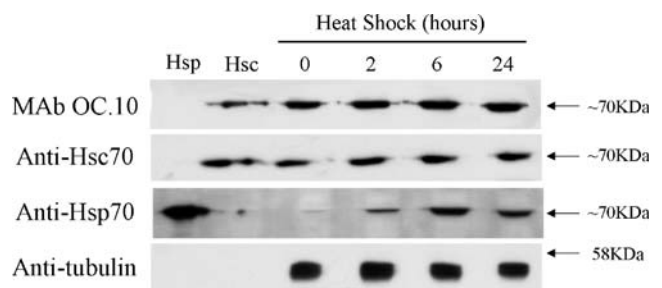


Fig. 6 Heat shock does not induce OC.10 antigen expression. Extracts prepared from rat BDE4 cells that were heat stressed at 42°C for 0, 2, 6, or 24 h were immunoblotted with the indicated antibody. Anti- α -tubulin was used as a loading control for cell lysates and was observed to react at a lower molecular weight than described by the supplier for mouse (~60 kDa) and gerbil (57 kDa). OC.10 antigen shows a similar expression profile as the constitutively expressed Hsc70 protein. Hsp70 protein shows inducible expression kinetics in response to heat shock. Recombinant Hsp70 (*Hsp*) and Hsc70 (*Hsc*) protein were loaded as controls (0.1 μ g/lane). Five micrograms of total cell lysate was loaded per lane

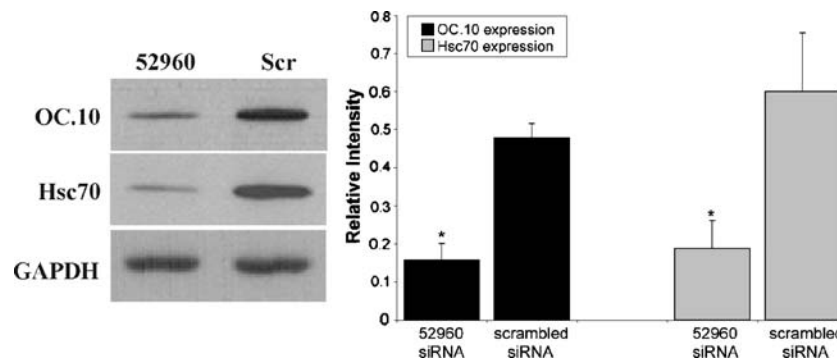


Fig. 7 Hsc70 siRNA decreases OC.10 antigen expression levels. BDE4 cells were nucleofected with Hsc70-specific siRNAs (201029, 52780, 52960) or negative control siRNA (scrambled) using the Amaxa system as described under “Materials and methods.” The siRNA knockdown effects were examined by immunoblot analysis 72 h post-nucleofection using MAb OC.10 and anti-Hsc70 (SPA-815) antibody. Ten micrograms of total cell lysate was loaded per lane. The

anti-GAPDH antibody was used as a loading control for the cell lysates. Immunoblot analysis demonstrated that Hsc70 siRNA 52960 provides highly efficient knockdown of Hsc70 and OC.10 expression levels (52960) as compared with the scrambled siRNA control (*Scr*). One representative experiment of three is shown. Mean±SEM of three separate experiments is graphed. * $P < 0.05$ versus scrambled siRNA nucleofection

Biotinylation of BDE4 cell surface proteins

To confirm biochemically that MAb OC.10 recognized a cell surface form of Hsc70, BDE4 surface proteins were labeled with sulfo-NHS-LC-LC biotin, a water-soluble reagent that

does not cross intact plasma membranes. Biotinylated proteins immunoprecipitated with neutravidin beads were analyzed by Western blot. As shown in Fig. 9, both MAb OC.10 and anti-Hsc70 detected a biotinylated protein with a molecular weight of approximately 70 kDa in the

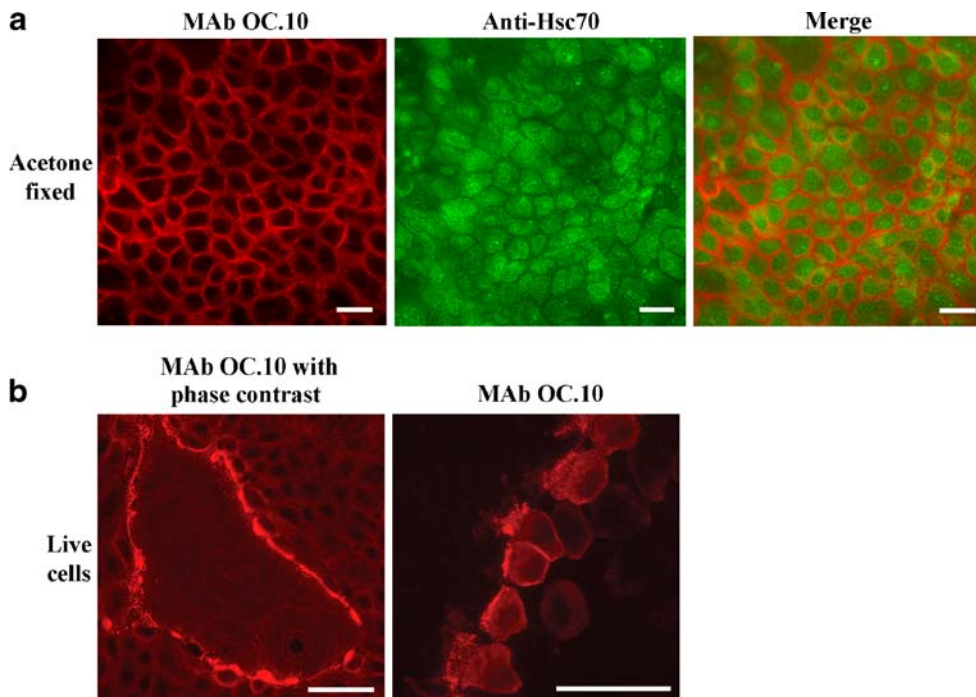


Fig. 8 Immunofluorescent distribution of the OC.10 antigen and Hsc70 protein on cultured BDE4 cells. **a** Acetone-fixed BDE4 cells co-labeled with MAb OC.10 and monoclonal anti-Hsc70 antibodies. MAb OC.10 exhibited strong cell surface and low cytoplasmic reactivity while the commercially available monoclonal anti-Hsc70 antibody showed strong cytoplasmic but no detectable plasma membrane reactivity. **b** Immunofluorescent labeling of live, non-

permeabilized BDE4 cells with MAb OC.10. Combined fluorescence and phase contrast shows MAb OC.10 reactivity is limited to cells at the leading edge of expanding colonies and is not apparent in areas of confluence. Localization of MAb OC.10 is polarized towards the outer apical membrane surface of live BDE4 cells. Scale bars represent 25 μm

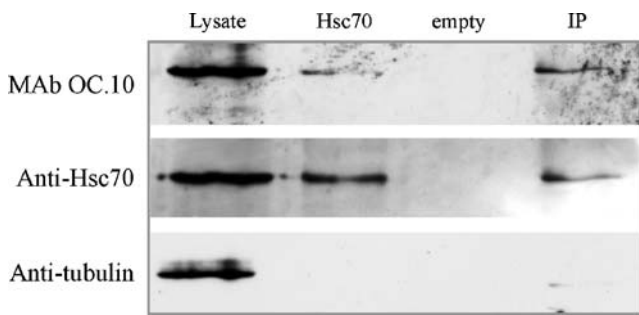


Fig. 9 Cell surface biotinylation of cultured BDE4 cells. Live BDE4 cells were incubated in PBS containing Sulfo-NHS-LC-LC biotin to label all cell surface proteins. Cells were harvested and incubated with immobilized neutravidin beads to precipitate biotinylated surface proteins. Immunoblot analysis with MAb OC.10 and anti-Hsc70 detected OC.10 antigen and Hsc70 protein, respectively in total cell extract (*Lysate*) and the neutravidin precipitated fraction (*IP*). Recombinant Hsc70 protein (*Hsc70*, 100 ng) was loaded as a positive control. The anti- α -tubulin immunoblot showed that α -tubulin, a known cytoplasmic protein, was not immunoprecipitated from the pool of biotinylated protein

neutravidin immunoprecipitated (IP) fraction. Cytosolic α -tubulin was detected in total lysate but was not present in the neutravidin bound fraction, demonstrating that cytosolic proteins were not biotinylated. To further confirm surface expression of Hsc70, a 70-kDa Gelcode Blue stained band of the surface biotinylated protein examined in Fig. 9 was excised, digested with trypsin, and analyzed by mass spectrometry. As shown in Table 2, LC-ESI-MS/MS analysis identified ten peptides that matched rat Hsc70 (gi 56385) with >99% confidence. In total, 17 Hsc70 peptides were identified that represented 37% of the Hsc70 protein sequence. These results demonstrate that a portion of the total pool of rat Hsc70 is expressed on the cell surface of rat BDE4 cells. In support of this finding, surface Hsc70 (gi 56385) was recently identified in purified plasma membrane preparations of the hepatocellular carcinoma cell line 253-NT-V (Lawson et al. 2006), suggesting that surface Hsc70 expression may be a more general phenomenon than previously appreciated.

Epitope mapping of MAb OC.10

Although prior observations demonstrating cell surface localization of Hsc70 have been reported (Tsuboi et al. 1994; Hirai et al. 1998; Fishelson et al. 2001), little is known regarding the orientation of the protein at the cell surface. Furthermore, the morphogenic changes induced in situ by MAb OC.10 (Fig. 1) suggest that the reactive epitope is located in a functional domain that is activated by antibody binding. To characterize the epitope recognized by MAb OC.10, purified antibody was used to screen a phage display dodecapeptide library. After three rounds of

selection and amplification, ten clones were randomly selected for DNA sequencing and the amino acid sequence of the inserts deduced. As shown in Table 3, five peptides with the sequence DYPTSSTAQPLP contained three residues (underlined) that aligned with amino acids 371 (Y), 377 (A), and 380 (L) that correspond to the N-terminal domain of Hsc70. Four additional peptides with the sequence TYCYPIHP[X]LLS contained two residues that aligned with amino acids 371 (Y) and 380 (L) of the same region. Although BLAST analysis did not identify these sequences as Hsc70, the conserved alignment of the underlined residues suggested that they might be part of the reactive epitope. To further evaluate the significance of this localization, region 340–410 of Hsc70 was reproduced by the PepSPOTS approach using overlapping arrays of 13 amino acid peptides offset by two and tested for their immunoreactivity against purified HRP-conjugated MAb OC.10. Strong reactivity mapped to peptides 1–8 and 15–17 that correspond to amino acids 340–366 and 368–384, respectively (Fig. 10 and Table 4). This is consistent with data obtained by phage display as the amino acids 371 (Y), 377 (A), and 380 (L) map to peptides 15 and 16 (Table 4). This pattern of immunoreactivity indicates that the surface

Table 2 Identification of *Rattus norvegicus* cell surface Hsc70 by mass spectrometry

Peptide sequence	Confidence (%)	Δ Mass (Da)
³⁰⁰ ARFEELNADLFR ³¹¹	99	-0.03
⁸⁹ HWPFOVNDAGRPK ¹⁰²	99	0.00
⁵⁷ NQVAONPTNTVFDK ⁷¹	99	0.02
⁵⁴⁰ NSLESYAFNMK ⁵⁵⁰	99	0.01
⁴²⁴ QTQFTFTYSDNQPGVLIQVYEGE ⁴⁴⁷	99	0.04
³⁶² SINPDEAVAYGAAVQAAILSGDK ³⁸⁴	99	0.04
²²¹ STAGDTHLGGEDFDNR ²³⁶	99	-0.12
³⁷ TTPSYVAFTDTER ⁴⁹	99	0.01
¹³⁸ TVTNAVVTVPAYFNDSQR ¹⁵⁵	99	-0.03
¹⁶⁰ DAGTIAGLNVL ¹⁷¹	86	-0.01
²³⁸ OVNHFAIEFK ²⁴⁶	67	-0.03
⁵⁷⁵ BNEIISWLDK ⁵⁸³	40	-0.03
⁴⁵⁹ FELTGIPPAPR ⁴⁶⁹	39	0.00
³⁴⁹ LLQDFENGK ³⁵⁷	39	0.02
¹¹³ SFYPEEVSSOVLT ¹²⁶	17	0.01
³²⁹ SQIHDIVLGGSTR ³⁴²	6	0.02
¹⁷² IINEPTAAAIAAYGLDK ¹⁸⁷	1	-0.01

Ions assigned to *Rattus norvegicus* Hsc70 peptides (gi 56385), based on agreement between theoretical and experimental fragmentation patterns, are listed by decreasing peptide confidence. The “ Δ Mass” column shows the mass error (experimental–theoretical mass) for the parental ion

O oxidized methionine, B carboxamidomethyl-cysteine

Table 3 Amino acid similarities between phage clones and Hsc70 (amino acids 370–381)

Protein origin	Sequence
Hsc70 (aa 370–381)	AYGAAVQA <u>AILS</u>
Phage clones 1–5	DYPTSS <u>TAQPLP</u>
Phage clones 6–9	TYCYPIHP[X] <u>LLS</u>

Underlined amino acids correspond to similarities between Hsc70 and sequenced phage. The [X] represents a nonspecific reading frame that did not code for an amino acid

specific epitope for MAb OC.10 resides in the N-terminal 340–384 amino acids of the ATPase domain of rat Hsc70.

Discussion

Previous work from our laboratory described the production of a panel of monoclonal antibodies reactive with bile duct and hepatic progenitor (oval cells in rodents) surface antigens. One such antibody, MAb OC.10, has been shown to recognize an epitope shared by fetal liver ductal cells, oval cells, mature bile duct cells (cholangiocytes), and hepatocellular carcinomas with oval cell characteristics but not by hepatocytes (Hixson et al. 2000). Because of its restricted surface expression profile, MAb OC.10 has been used in combination with other lineage-specific antibodies to isolate antigenically defined subpopulations present during liver development, renewal, and carcinogenesis (Simper-Ronan et al. 2006). In the present study, we have shown that intrasplenic injection of MAb OC.10 into newborn rat pups strongly labels intrahepatic bile duct cells also positive for the bile duct marker OV-6. Interestingly, the in situ labeling of OV-6-positive cholangiocytes by MAb OC.10 promoted the morphogenesis of well-defined bile duct structures relative to isotype-injected control animals. Since this finding was of particular interest, we designed a protocol for purifying OC.10 from isolated rat biliary tree and identified the protein recognized by MAb OC.10 as the constitutively expressed 70-kDa heat shock cognate protein, Hsc70. The reactive epitope for MAb

Table 4 MAb OC.10-reactive peptide sequences corresponding to Hsc70 PepSpots membrane spanning amino acids 340–410

Binding region	Amino acid sequence
Region 1 (aa 340–366)	STRIPKIQKLLQDFNKGKELNKSINPD
1. aa 340–352	STRIPKIQKLLQD
2. aa 342–354	RIPKIQKLLQDF
3. aa 344–356	PKIQKLLQDFNKG
4. aa 346–358	IQKLLQDFNKGKE
5. aa 348–360	KLLQDFNKGKELN
6. aa 350–362	LQDFNKGKELNKS
7. aa 352–364	DFNKGKELNKSIN
8. aa 354–366	FNGKELNKSINPD
Region 2 (aa 368–378)	AVAYGAAVQA <u>AILS</u> SGDK
15. aa 368–380	AVAYGAAVQA <u>AIL</u> ^a
16. aa 370–382	AYGAAVQA <u>AILS</u> G ^a
17. aa 372–384	GAAVQA <u>AILS</u> SGDK ^a

^a The underlined amino acids (aa) correspond to residues defined by phage display

OC.10 was mapped to the 340–384 stretch of amino acids showing that this region of the Hsc70 ATPase domain is exposed when presented on the cell surface. Moreover, we have previously reported that OC.10 is expressed by a subset of rat primary HCC that co-express other oval/ductal cell markers, a finding that suggested the OC.10 epitope was exposed on the surface of HCC derived from oval cell progenitors (Hixson et al. 2000). Taken together, these data indicate that Hsc70 has the potential to be expressed on the surface of certain tumor cells.

The Hsc70 protein, also known as heat shock cognate 73 (Hsc73), is a member of the heat shock protein 70 (HSP70) family (Sorger and Pelham 1987; De Maio 1999), a family of proteins ranging in size between 66 and 78 kDa. Members of the HSP70 family have three structural and functional domains: a 44-kDa N-terminal ATPase domain (residues 1–384), an 18-kDa protein binding domain (residues 385–543), and a 10-kDa variable domain (residues 544–646) that binds co-chaperone proteins (Mayer and Bukau 2005). Proteins of the HSP70 family, including Hsc70, have been shown to function as intracellular chaperones with essential roles in protein synthesis, folding and assembly, trafficking, and degradation (Daugaard et al. 2007). Hsc70 has also been implicated in various stages of clatherin-mediated endocytosis (Schlossman et al. 1984; Newmyer et al. 2003; Eisenberg and Greene 2007), antigen presentation (Zhou et al. 2005; Kamiguchi et al. 2008), and protection from apoptosis (de la Rosa et al. 1998; Dastoor and Dreyer 2000).

To the best of our knowledge, this is the first report to define a cell surface Hsc70 epitope exposed in situ on the surface of cholangiocytes and oval cells but not on

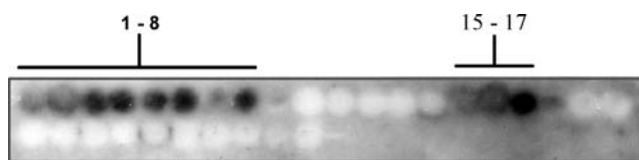


Fig. 10 The MAb OC.10 epitope maps to the N-terminal ATPase domain of Hsc70. A membrane containing an overlapping series of 13 amino acid peptides that spanned region 340–410 of rat Hsc70 was used to define the epitope recognized by purified HRP-conjugated MAb OC.10. MAb OC.10 reacted strongly with PepSPOTS 1–8 and 15–17 that correspond to amino acids 340–366 and 368–384, respectively

hepatocytes. Although there have been previous reports describing cell surface expression (Tsuboi et al. 1994; Hirai et al. 1998; Fishelson et al. 2001), little is known regarding the orientation of Hsc70 in the plasma membrane or how this well-described cytoplasmic protein localizes to the cell surface. Previously, Hirai et al. (1998) identified a monoclonal antibody that recognized an epitope spanning amino acid residues 350–372 of the Hsc70 ATPase domain and confirmed by FACS analysis that this reactive epitope was expressed on the surface of Daudi cells. This is highly consistent with our current mapping data that places the reactive epitope for MAb OC.10 in a similar region that spans residues 340–384 of the Hsc70 ATPase domain. However, surface-exposed epitopes of Hsc70 may not be limited to the ATPase domain. Fishelson and colleagues used four different antibodies to define surface exposed epitopes located in the N-terminal ATPase domain and C-terminal peptide binding domain of Hsc70 on complement-stressed human K562 cells (Fishelson et al. 2001). Although the two antibodies directed against the N-terminal domain also reacted with Hsp70, the C-terminal antibodies were specific for Hsc70. Interestingly, surface reactivity with one of these C-terminal reactive antibodies, the commercially available SPA-816 (residues 556–568), exhibited primarily cytoplasmic staining when tested against our BDE cell lines (data not shown), suggesting that the presentation of extracellular Hsc70 domains may vary between different cell types.

In contrast to Hsc70, cell surface expression of Hsp70 has been well described on various tumor cell types (Ferrarini et al. 1992; Multhoff et al. 1995; Shin et al. 2003). Multhoff and colleagues have further demonstrated that the exposed extracellular domain of Hsp70 expressed on the surface of human colon carcinoma cells was situated in the C-terminal substrate binding domain and that this extracellular domain was associated with increased proliferative and cytolytic natural killer (NK) cell activity (Botzler et al. 1996, 1998; Multhoff et al. 1997, 1999). More recently, peptide scanning mapped a surface-exposed Hsp70 epitope to residues 454–461 of the C-terminal domain, and a synthetic peptide corresponding to residues 450–463 was shown to stimulate the proliferation and cytolytic activity of NK cells at concentrations similar to those described for full-length Hsp70 protein. Although the corresponding region for Hsc70 is highly homologous, Hsc70 failed to elicit a similar NK cell response (Multhoff et al. 2001).

Despite the high degree of similarity between Hsc70 and Hsp70, it has been possible to differentiate between these two proteins. It was shown by immunoblot analysis that MAb OC.10 reacted specifically with recombinant Hsc70 protein and did not show affinity for recombinant Hsp70 protein. Consistent with this specificity, heat shock treat-

ment did not upregulate OC.10 or Hsc70 expression in treated BDE cells. Importantly, siRNA-mediated knock-down of Hsc70 expression resulted in decreased OC.10 expression in nucleofected BDE cells. The reduced reactivity of MAb OC.10 with immunoblots in comparison to the commercially available anti-Hsc70 antibody SPA-815 suggested that MAb OC.10 was either recognizing a subfraction of the total pool of Hsc70 protein or was displaying reduced affinity towards the denatured form of the protein. However, in immunofluorescence assays, MAb OC.10 reactivity was restricted to the cell surface and showed little reactivity with the more abundant pool of cytosolic Hsc70 recognized by SPA-815. Differences in immunofluorescence reactivity for MAb OC.10 were also observed between live and acetone fixed cells, with the latter displaying an abundant pool of surface Hsc70 and the former showing fluorescence limited to the plasma membrane at the outer edge of cell colonies. Although the significance of this finding is unclear at present, it suggests that the MAb OC.10 epitope in membrane areas of cell–cell contact is unmasked by acetone fixation, an indication that surface Hsc70 may be interacting directly with membrane lipids. Such an association has been previously shown for recombinant Hsc70 from its interaction with artificial phospholipid membranes that lead to the formation of nucleotide-dependent ion conducting channels (Arispe and De Maio 2000). The ability of both Hsc70 and Hsp70 to promote the aggregation of phosphatidylserine (PS) liposomes (Arispe et al. 2002) and to interact with PS on the surface of cultured PC12 cells (Arispe et al. 2004) provided further evidence for direct interactions with membrane lipids.

Hsp70 has also been shown to associate with lipid rafts (Broquet et al. 2003). These lipid-based organizational platforms, enriched in glycosphingolipids and cholesterol, are located in plasma membranes and have been implicated in a number of biological functions including membrane trafficking and signal transduction (Simons and Ikonen 1997; Hanzal-Bayer and Hancock 2007; Patra 2008). Interestingly, Multhoff and colleagues have recently shown that surface Hsp70 on human tumor cells interacts with globotriaosylceramide (Gb3), a glycosphingolipid associated with lipid rafts. Moreover, it was shown that binding of Hsp70 to artificial raft-like liposomes required the inclusion of Gb3 and further that depletion of ceramide-based glycosphingolipids, including Gb3, decreased Hsp70 surface presentation on tumor cells (Gehrmann et al. 2008). It will be interesting to determine if membrane lipid composition regulates surface Hsc70 epitope availability, as it may provide a possible explanation for the differences in MAb OC.10 reactivity between surface-reactive cholangiocytes and hepatocytes and for the heterogeneity of MAb OC.10 reactivity with hepatocellular carcinomas displaying oval

cell characteristics (Hixson et al. 2000). It is also tempting to speculate that the punctate staining pattern of MAb OC.10 by immunofluorescence represents Hsc70 in lipid rafts, a targeting site previously established for Hsp70. This would provide a plausible mechanism for regulating membrane-mediated signaling events involved in the observed morphogenic stimulus provided by the injected MAb OC.10.

Although much work remains in elucidating the biological function of surface Hsc70 on oval and bile duct epithelial cells, it is possible to propose candidate functions based on known characteristics of the HSP70 proteins. For example, as a well-described chaperone, it is likely that Hsc70 transports proteins to the cell surface where it is also required for the proper folding of associated membrane proteins. It is also plausible that Hsc70 is required for recycling of surface proteins and targets them for proteosomal degradation. Hsc70 has also been implicated in various differentiation and developmental processes (de la Rosa et al. 1998; Elefant and Palter 1999; Vega-Nunez et al. 1999; Shrivastav et al. 2008), a finding consistent with its involvement as an active component of survival and proliferation pathways. As reported here, studies initially designed to label OC.10 expressing cells *in situ* for cell isolation schemes for lineage analysis demonstrated that binding of MAb OC.10 administered by intrasplenic injection promoted a change in bile duct morphology. Although the mechanism for this effect is at present unclear, the results suggest that binding of MAb OC.10 to surface Hsc70 is stimulating morphogenic signaling pathways. Supporting this assumption is an emerging regulatory role for Hsc70 in cell signaling, a role suggested by signaling complexes composed of Hsc70 and CXCR4 (Triantafilou et al. 2001), CXCR2 (Fan et al. 2002), and the G protein-coupled A1 adenosine receptor (Sarrio et al. 2000). Hsc70 binding has also been shown to be required for the activation of glucocorticoid receptors in the presence of steroids (Rajapandi et al. 2000).

It will be critical to determine if the reported morphogenic response to MAb OC.10 is epitope-dependent. If so, it is tempting to speculate that MAb OC.10 mimics a natural ligand that interacts with the cell surface-exposed epitope of Hsc70 to regulate signaling pathways critical to growth and survival. Dysregulation of surface Hsc70 or its natural ligands could therefore contribute to the development and progression of progenitor-derived liver cancers including hepatocellular carcinoma and cholangiocarcinomas originating from mature bile duct cells. Furthermore, the identification of normal signaling pathways in response to MAb OC.10 may contribute to our understanding and identification of parallel pathways shared by tumor cells responding to stress stimuli in the neoplastic microenvironment. In summary, establishing an identity between OC.10

and Hsc70 provides an essential step towards defining the significance of this surface marker in the differentiation and function of cholangiocytes and intrahepatic bile ducts during liver development and carcinogenesis.

Acknowledgments We wish to thank Laura Bangs and Sandy DeAngelis for clerical assistance and Dr. James G. Clifton for technical assistance with the QSTAR XL mass spectrometry studies. This work was supported by grants CA93840, CA42715, and RRP20RR017695 (to D.C.H.) from the National Institutes of Health and RI-INBRE Grant P20RR016457 (to D.R.M.) from the National Center for Research Resources (NCRR), a component of the National Institutes of Health (NIH). Its contents are solely the responsibility of the authors and do not necessarily represent the official views of NCRR or NIH.

References

- Arispe N, De Maio A (2000) ATP and ADP modulate a cation channel formed by Hsc70 in acidic phospholipid membranes. *J Biol Chem* 275:30839–30843. doi:10.1074/jbc.M005226200
- Arispe N, Doh M, De Maio A (2002) Lipid interaction differentiates the constitutive and stress-induced heat shock proteins Hsc70 and Hsp70. *Cell Stress Chaperones* 7:330–338. doi:10.1379/1466-1268(2002)007<0330:LIDTCA>2.0.CO;2
- Arispe N, Doh M, Simakova O, Kurganov B, De Maio A (2004) Hsc70 and Hsp70 interact with phosphatidylserine on the surface of PC12 cells resulting in a decrease of viability. *FASEB J* 18:1636–1645. doi:10.1096/fj.04-2088com
- Bisgaard HC, Parmelee DC, Dunsford HA, Sechi S, Thorgeirsson SS (1993) Keratin 14 protein in cultured nonparenchymal rat hepatic epithelial cells: characterization of keratin 14 and keratin 19 as antigens for the commonly used mouse monoclonal antibody OV-6. *Mol Carcinog* 7:60–66. doi:10.1002/mc.2940070110
- Botzler C, Issels R, Multhoff G (1996) Heat-shock protein 72 cell-surface expression on human lung carcinoma cells is associated with an increased sensitivity to lysis mediated by adherent natural killer cells. *Cancer Immunol Immunother* 43:226–230. doi:10.1007/s002620050326
- Botzler C, Li G, Issels RD, Multhoff G (1998) Definition of extracellular localized epitopes of Hsp70 involved in an NK immune response. *Cell Stress Chaperones* 3:6–11. doi:10.1379/1466-1268(1998)003<0006:DOELEO>2.3.CO;2
- Broquet AH, Thomas G, Masliah J, Trugnan G, Bachelet M (2003) Expression of the molecular chaperone Hsp70 in detergent-resistant microdomains correlates with its membrane delivery and release. *J Biol Chem* 278:21601–21606. doi:10.1074/jbc.M302326200
- Clifton JG, Brown MK, Huang F et al (2006) Identification of members of the annexin family in the detergent-insoluble fraction of rat Morris hepatoma plasma membranes. *J Chromatogr A* 1123:205–211. doi:10.1016/j.chroma.2006.02.020
- Coleman W, McCullough K, Esch G, Faris R, Hixson D, Smith G, Grisham J (1997) Evaluation of the differentiation potential of WB-F344 rat liver epithelial stem-like cells *in vivo*: differentiation to hepatocytes following transplantation into dipeptidylpeptidase IV-deficient rat liver. *Am J Pathol* 151:353–359
- Dabeva MD, Hwang SG, Vasa SR et al (1997) Differentiation of pancreatic epithelial progenitor cells into hepatocytes following

- transplantation into rat liver. *Proc Natl Acad Sci U S A* 94:7356–7361. doi:10.1073/pnas.94.14.7356
- Dastoor Z, Dreyer J (2000) Nuclear translocation and aggregate formation of heat shock cognate protein 70 (Hsc70) in oxidative stress and apoptosis. *J Cell Sci* 113(Pt 16):2845–2854
- Daugaard M, Rohde M, Jaattela M (2007) The heat shock protein 70 family: highly homologous proteins with overlapping and distinct functions. *FEBS Lett* 581:3702–3710. doi:10.1016/j.febslet.2007.05.039
- de la Rosa EJ, Vega-Nunez E, Morales AV, Serma J, Rubio E, de Pablo F (1998) Modulation of the chaperone heat shock cognate 70 by embryonic (pro) insulin correlates with prevention of apoptosis. *Proc Natl Acad Sci U S A* 95:9950–9955. doi:10.1073/pnas.95.17.9950
- De Maio A (1999) Heat shock proteins: facts, thoughts, and dreams. *Shock* 11:1–12. doi:10.1097/00024382-199901000-00001
- Dunsford HA, Karnasuta C, Hunt JM, Sell S (1989) Different lineages of chemically induced hepatocellular carcinoma in rats defined by monoclonal antibodies. *Cancer Res* 49:4894–4900
- Eisenberg E, Greene LE (2007) Multiple roles of auxilin and hsc70 in clathrin-mediated endocytosis. *Traffic* 8:640–646. doi:10.1111/j.1600-0854.2007.00568.x
- Elefant F, Palter KB (1999) Tissue-specific expression of dominant negative mutant *Drosophila* HSC70 causes developmental defects and lethality. *Mol Biol Cell* 10:2101–2117
- Fan GH, Yang W, Sai J, Richmond A (2002) Hsc/Hsp70 interacting protein (hip) associates with CXCR2 and regulates the receptor signaling and trafficking. *J Biol Chem* 277:6590–6597. doi:10.1074/jbc.M110588200
- Ferrarini M, Heltai S, Zocchi MR, Rugarli C (1992) Unusual expression and localization of heat-shock proteins in human tumor cells. *Int J Cancer* 51:613–619. doi:10.1002/ijc.2910510418
- Fishelson Z, Hochman I, Greene LE, Eisenberg E (2001) Contribution of heat shock proteins to cell protection from complement-mediated lysis. *Int Immunol* 13:983–991. doi:10.1093/intimm/13.8.983
- Gehrmann M, Liebisch G, Schmitz G et al (2008) Tumor-specific Hsp70 plasma membrane localization is enabled by the glycosphingolipid Gb3. *PLoS ONE* 3:e1925
- Gordon GJ, Coleman WB, Grisham JW (2000) Temporal analysis of hepatocyte differentiation by small hepatocyte-like progenitor cells during liver regeneration in retrorsine-exposed rats. *Am J Pathol* 157:771–786
- Hanzal-Bayer MF, Hancock JF (2007) Lipid rafts and membrane traffic. *FEBS Lett* 581:2098–2104. doi:10.1016/j.febslet.2007.03.019
- Hirai I, Sato N, Qi W, Ohtani S, Torigoe T, Kikuchi K (1998) Localization of pN22 70 kDa heat shock cognate-like protein in the plasma membrane. *Cell Struct Funct* 23:153–158
- Hixson DC, Fowler LC (1997) Development and phenotypic heterogeneity of intrahepatic biliary epithelial cells. In: Sirica AE, Longnecker DS (eds) *Biliary and pancreatic ductal epithelium*. Marcel Dekker, New York, pp 1–40
- Hixson DC, Brown J, McBride AC, Affigne S (2000) Differentiation status of rat ductal cells and ethionine-induced hepatic carcinomas defined with surface-reactive monoclonal antibodies. *Exp Mol Pathol* 68:152–169. doi:10.1006/exmp.2000.2302
- Kamiguchi K, Torigoe T, Fujiwara O et al (2008) Disruption of the association of 73 kDa heat shock cognate protein with transporters associated with antigen processing (TAP) decreases TAP-dependent translocation of antigenic peptides into the endoplasmic reticulum. *Microbiol Immunol* 52:94–106. doi:10.1111/j.1348-0421.2008.00017.x
- Kubota H, Reid LM (2000) Clonogenic hepatoblasts, common precursors for hepatocytic and biliary lineages, are lacking classical major histocompatibility complex class I antigen. *Proc Natl Acad Sci U S A* 97:12132–12137. doi:10.1073/pnas.97.22.12132
- Lawson EL, Clifton JG, Huang F, Li X, Hixson DC, Josic D (2006) Use of magnetic beads with immobilized monoclonal antibodies for isolation of highly pure plasma membranes. *Electrophoresis* 27:2747–2758. doi:10.1002/elps.200600059
- Mayer MP, Bukau B (2005) Hsp70 chaperones: cellular functions and molecular mechanism. *Cell Mol Life Sci* 62:670–684. doi:10.1007/s00018-004-4464-6
- Multhoff G, Botzler C, Wiesnet M, Muller E, Meier T, Wilmanns W, Issels RD (1995) A stress-inducible 72-kDa heat-shock protein (HSP72) is expressed on the surface of human tumor cells, but not on normal cells. *Int J Cancer* 61:272–279. doi:10.1002/ijc.2910610222
- Multhoff G, Botzler C, Jennen L, Schmidt J, Ellwart J, Issels R (1997) Heat shock protein 72 on tumor cells: a recognition structure for natural killer cells. *J Immunol* 158:4341–4350
- Multhoff G, Mizzen L, Winchester CC et al (1999) Heat shock protein 70 (Hsp70) stimulates proliferation and cytolytic activity of natural killer cells. *Exp Hematol* 27:1627–1636. doi:10.1016/S0301-472X(99)00104-6
- Multhoff G, Pfister K, Gehrmann M, Hantschel M, Gross C, Hafner M, Hiddemann W (2001) A 14-mer Hsp70 peptide stimulates natural killer (NK) cell activity. *Cell Stress Chaperones* 6:337–344. doi:10.1379/1466-1268(2001)006<0337:AMHPSN>2.0.CO;2
- Newmyer SL, Christensen A, Sever S (2003) Auxilin–dynamin interactions link the uncoating ATPase chaperone machinery with vesicle formation. *Dev Cell* 4:929–940. doi:10.1016/S1534-5807(03)00157-6
- Novikoff PM, Yam A, Oikawa I (1996) Blast-like cell compartment in carcinogen-induced proliferating bile ductules. *Am J Pathol* 148:1473–1492
- Patra SK (2008) Dissecting lipid raft facilitated cell signaling pathways in cancer. *Biochim Biophys Acta* 1785:182–206
- Rajapandi T, Greene LE, Eisenberg E (2000) The molecular chaperones Hsp90 and Hsc70 are both necessary and sufficient to activate hormone binding by glucocorticoid receptor. *J Biol Chem* 275:22597–22604. doi:10.1074/jbc.M002035200
- Sarrio S, Casado V, Escrache M et al (2000) The heat shock cognate protein hsc73 assembles with A(1) adenosine receptors to form functional modules in the cell membrane. *Mol Cell Biol* 20:5164–5174. doi:10.1128/MCB.20.14.5164-5174.2000
- Schlossman DM, Schmid SL, Braell WA, Rothman JE (1984) An enzyme that removes clathrin coats: purification of an uncoating ATPase. *J Cell Biol* 99:723–733. doi:10.1083/jcb.99.2.723
- Sell S (1998) Comparison of liver progenitor cells in human atypical ductular reactions with those seen in experimental models of liver injury. *Hepatology* 27:317–331. doi:10.1002/hep.510270202
- Sell S, Ilic Z (eds) (1997) *Response to injury. Liver stem cells*. Landes Company, Austin, 223–286
- Sell S, Pierce GB (1994) Maturation arrest of stem cell differentiation is a common pathway for the cellular origin of teratocarcinomas and epithelial cancers. *Lab Invest* 70:6–22
- Shin BK, Wang H, Yim AM et al (2003) Global profiling of the cell surface proteome of cancer cells uncovers an abundance of proteins with chaperone function. *J Biol Chem* 278:7607–7616. doi:10.1074/jbc.M210455200
- Shrivastav A, Varma S, Lawman Z et al (2008) Requirement of N-myristoyltransferase 1 in the development of monocytic lineage. *J Immunol* 180:1019–1028
- Simons K, Ikonen E (1997) Functional rafts in cell membranes. *Nature* 387:569–572. doi:10.1038/42408
- Simper-Ronan R, Brilliant K, Flanagan D, Carreiro M, Callanan H, Sabo E, Hixson DC (2006) Cholangiocyte marker-positive and -negative fetal liver cells differ significantly in their ability to regenerate the livers of adult rats exposed to retrorsine. *Development* 133:4269–4279. doi:10.1242/dev.02589

- Sorger PK, Pelham HR (1987) Cloning and expression of a gene encoding hsc73, the major hsp70-like protein in unstressed rat cells. *Embo J* 6:993–998
- Suzuki A, Zheng YY, Kaneko S, Onodera M, Fukao K, Nakauchi H, Taniguchi H (2002) Clonal identification and characterization of self-renewing pluripotent stem cells in the developing liver. *J Cell Biol* 156:173–184. doi:10.1083/jcb.200108066
- Tateno C, Yoshizato K (1996) Growth and differentiation in culture of clonogenic hepatocytes that express both phenotypes of hepatocytes and biliary epithelial cells. *Am J Pathol* 149:1593–1605
- Tavaria M, Gabriele T, Kola I, Anderson RL (1996) A hitchhiker's guide to the human Hsp70 family. *Cell Stress Chaperones* 1:23–28. doi:10.1379/1466-1268(1996)001<0023:AHSGTT>2.3.CO;2
- Triantafilou K, Triantafilou M, Dedrick RL (2001) A CD14-independent LPS receptor cluster. *Nat Immunol* 2:338–345. doi:10.1038/86342
- Tsuboi N, Ishikawa M, Tamura Y et al (1994) Monoclonal antibody specifically reacting against 73-kilodalton heat shock cognate protein: possible expression on mammalian cell surface. *Hybridoma* 13:373–381
- Tsukahara F, Maru Y (2004) Identification of novel nuclear export and nuclear localization-related signals in human heat shock cognate protein 70. *J Biol Chem* 279:8867–8872. doi:10.1074/jbc.M308848200
- Vega-Nunez E, Pena-Melian A, de la Rosa EJ, de Pablo F (1999) Dynamic restricted expression of the chaperone Hsc70 in early chick development. *Mech Dev* 82:199–203. doi:10.1016/S0925-4773(99)00015-5
- Yang L, Faris RA, Hixson DC (1993a) Characterization of a mature bile duct antigen expressed on a subpopulation of biliary ductular cells but absent from oval cells. *Hepatology* 18:357–366
- Yang L, Faris RA, Hixson DC (1993b) Long-term culture and characteristics of normal rat liver bile duct epithelial cells. *Gastroenterology* 104:840–852
- Zhou D, Li P, Lin Y et al (2005) Lamp-2a facilitates MHC class II presentation of cytoplasmic antigens. *Immunity* 22:571–581. doi:10.1016/j.immuni.2005.03.009